Inorg. Chem. **2007**, *46*, 1563–1574

A Series of New Organic–Inorganic Molybdenum Arsenate Complexes Based on $[(ZnO_6)(As_3O_3)_2Mo_6O_{18}]^{4-}$ and $[H_xAs_2Mo_6O_{26}]^{(6-x)-}$ Clusters as SBUs

Chunyan Sun, Yangguang Li, Enbo Wang,* Dongrong Xiao, Haiyan An, and Lin Xu

Key Laboratory of Polyoxometalate Science of Ministry of Education, Institute of Polyoxometalate Chemistry, Department of Chemistry, Northeast Normal University, Changchun, 130024, P. R. China

Received July 4, 2006

By synthesizing the novel molybdenum arsenate complexes, we have obtained eight new structures, namely, (4,4′-bipy)$[Zn(4,4'\text{-bipy})_2(H_2O)_2]_2[(ZnO_6)(As^{III}_3O_3)_2Mo_6O_{18}]\cdot 7H_2O$, **1**, $[Zn(phen)_2(H_2O)]_2[(ZnO_6)(As^{III}_3O_3)_2Mo_6O_{18}]\cdot 4H_2O$, **2**, $[Zn(2,2'\text{-bipy})_2(H_2O)]_2[(ZnO_6)(As^{III}_3O_3)_2Mo_6O_{18}]\cdot 4H_2O$, **3**, $[Zn(H4,4'\text{-bipy})_2(H_2O)_4][(ZnO_6)(As^{III}_3O_3)_2Mo_6O_{18}]\cdot 8H_2O$, **4**, $(H_24,4'\text{-bipy})[Cu^I(4,4'\text{-bipy})]_2[H_2As^V_2Mo_6O_{26}]\cdot H_2O$, **5**, $(H_24,4'\text{-bipy})_3[As^V_2Mo_6O_{26}]\cdot 4H_2O$, **6**, $(H_24,4'\text{-bipy})_3[As^V_2Mo_6O_{26}(H_2O)]\cdot 4H_2O$, **7**, and $(H_24,4'\text{-bipy})_{2.5}(H_3O)[As^V_2Mo_6O_{26}(H_2O)]\cdot 1.25H_2O$, **8** (4,4′-bipy = 4,4′-bipyridine, 2,2′-bipy = 2,2′-bipyridine, phen = 1,10-phenanthroline). These structures were determined by single-crystal X-ray diffraction analysis and were further characterized by elemental analysis, IR, XPS spectroscopy, and TG analysis. The structure of **1** is constructed from two-dimensional square gridlike sheets linked by the polyanions $[(ZnO_6)(As^{III}_3O_3)_2Mo_6O_{18}]^{4-}$ via hydrogen-bonding interactions to form a three-dimensional supramolecular framework with two types of channels. Compounds **2** and **3** display similar bisupported structures. Compound **4** features a three-dimensional supramolecular architecture. Compound **5** possesses a 1D infinite ladderlike ribbon. Compounds **6**–**8** are discrete structures exhibiting three isomeric forms of $[H_xAs_2Mo_6O_{26}]^{(6-x)-}$. Furthermore, compound **8** represents a new isomer B′-$[As_2Mo_6O_{26}(H_2O)]^{6-}$. In addition, the fluorescent properties of compounds **1**–**3** are reported.

Introduction

Polyoxometalates (POMs), an important class of inorganic compounds, have many properties that make them attractive for applications in catalysis, materials science, and medicine.[1–5] During the past few years, research on POMs has greatly spread and mighty endeavors have been devoted to prepare functionalized POM-based materials via incorporation or coordination of metal−organic units or organic moieties with catalysis, optical, electronic, and magnetic properties.[6–8]

Heteropolymolybdates are an important part in this field,[9,10] because of the redox-active nature of molybdenum. Such

* To whom correspondence should be addressed. E-mail: wangenbo@public.cc.jl.cn; wangeb889@nenu.edu.cn.

(1) (a) Pope, M. T. *Heteropoly and Isopoly Oxometalates*; Springer: Berlin, 1983. (b) Xiong, R. G.; You, X. Z.; Abrahams, B. F.; Xue, Z. L.; Che, C. M. *Angew. Chem., Int. Ed.* **2001**, *40*, 4422. (c) Li, J. R.; Bu, X. H.; Zhang, R. H. *Inorg. Chem.* **2004**, *43*, 237. (d) Cui, Y.; Ngo, H. L. White, P. S.; Lin, W. B. *Chem. Commun.* **2002**, 1666.

(2) (a) Hill, C. L.; McCartha, C. M. P. *Coord. Chem. Rev.* **1995**, *143*, 407. (b) Hill, C. F.; Zhuang, H. H.; Huang, J. S. *Chem. Commun.* **2003**, 1284. (d) Xu, B. B.; Peng, Z. H.; Wei, Y. G.; Powell, D. R. *Chem. Commun.* **2003,** 2562.

(3) (a) Fukaya, K.; Yamase, T. *Angew. Chem., Int. Ed.* **2003**, *42*, 654. (b) Shi, Z.; Feng, S.; Gao, S.; Zhang, L.; Yang, G.; Hua, J. *Angew. Chem., Int. Ed.* **2000**, *39*, 2325. (c) Zheng, S. L.; Yang, J. H.; Yu, X. L.; Chen, X. M.; Wong, W. T. *Inorg. Chem.* **2004**, *43*, 830.

(4) (a) Cui, X. B.; Xu, J. Q.; Meng, H.; Zheng, S. T.; Yang, G. Y. *Inorg. Chem.* **2004**, *43*, 8005. (b) Sun, C. Y.; Wang, E. B.; Xiao, D. R.; An, H. Y.; Xu, L. *J. Mol. Struct.* **2005**, *741*, 149. (c) Sun, C. Y.; Wang, E. B.; Xiao, D. R.; An, H. Y.; Xu, L. *Transition Met. Chem.* **2005**, *30*, 873.

(5) (a) Sadakane, M.; Dickman, M. H.; Pope, M. T. *Angew. Chem., Int. Ed.* **2000**, *39*, 2914. (b) Kortz, U.; Hamzeh, S. S.; Nasser, N. A. *Chem.—Eur. J.* **2003**, *9*, 2945. (c) Wang, Y.; Yu, J. H.; Guo, M.; Xu, R. R. *Angew. Chem., Int. Ed.* **2003**, *42*, 4089.

(6) (a) *Polyoxometalate Chemistry: From Topology Via Self-Assembly to Applications;* Pope, M. T., Müller, A., Eds. Kluwer: Dordrecht, The Netherlands, 2001. (b) Müller, A.; Döring, J. *Angew. Chem., Int. Ed. Engl.* **1988**, *27*, 1721. (c) Bi, L. H.; Dickman, M. H.; Kortz, U.; Dix, I. *Chem. Commun.* **2005**, 3962.

(7) (a) Kortz, U.; Nellutla, S.; Stowe, A. C.; Dalal, N. S.; Tol, J. V.; Bassil, B. S. *Inorg. Chem.* **2004**, *43*, 144. (b) Wu, C. D.; Lu, C. Z.; Chen, S. M.; Zhuang, H. H.; Huang, J. S. *Polyhedron.* **2003**, *22*, 3091. (c) Xiao, D. R.; Li, Y. G.; Wang, E. B.; Wang, S. T.; Hou, Y.; De, G. J. H.; Hu, C. W. *Inorg. Chem.* **2003**, *42*, 7652.

(8) (a) Dumas, E.; Livage, C.; Halut, S.; Hervé, G. *Chem. Commun.* **1996**, 243. (b) An, H. Y.; Wang, E. B.; Xiao, D. R.; Li, Y. G.; Wang, X. L.; Xu, L. *Angew. Chem., Int. Ed.* **2005**, *5*, 854. (c) An, H. Y.; Li, Y. G.; Wang, E. B.; Xiao, D. R.; Sun, C. Y; Xu, L. *Inorg. Chem.* **2005**, *44*, 6201.

10.1021/ic061227j CCC: $37.00
Published on Web 02/03/2007

polymolybdates could be molecularly fine-tuned and provide potential new types of catalyst systems, as well as interesting functionalized materials with other properties. Until now, a large number of new functionalized materials based on molybdenum phosphates have been synthesized, and they have exhibited not only varieties of novel frameworks but also many applications in catalysis, ion exchange, and molecular sieves,[11−13] which have been reviewed by Haushalter and co-workers.[11a]

In contrast to the rich information on solid materials based on molybdenum phosphates, the arsenate analogues remain relatively undeveloped. So far the reports on molybdenum arsenates have been mainly concentrated on several discrete molybdenum arsenate clusters.[14−15] Only recently, an interesting systemic study on extended structures based on molybdenum organoarsonate have been performed by Zubieta and his co-workers,[16] and the use of inorganic molybdearsenate clusters as SBUs to construct extended structures still seldom has been reported.[16a] However, solid materials based on molybdenum arsenates may possess many potential applications in catalysis and materials science.[15c,17] For instance, molybdenum arsenates can act as functionalized materials to be used as coatings on carbon steel improved its corrosion resistance.[17a] In addition, metal arsenates are of interest for their applications as catalysts, nonlinear optical materials, and ion exchangers,[18] and the synthesis of metal arsenates is an effective technique in the immobilization mine tailings.[19] Therefore, further research is necessary to enrich and develop this branch. So we made an effort to obtain new materials based on inorganic molybdenum arsenate building units with novel structures and interesting properties and then further investigate their final applications in material science because only an elaborate structural comprehending of functionalized material permits rational investigation of applications.

Recently, one of the important avenues in the design of new functionalized materials based on POMs has been put forward by Zubieta and Khan et al.;[20] they combined secondary transition metal complexes (TMCs) and POMs via molecular assemblies to produce TMC-linked POMs or POM-supported TMCs. So our synthetic strategy is the introduction of secondary metal−organic complexes, which serve as organic−inorganic bridging fragments to link the discrete As−Mo−O motif forming extended and supported structures. Moreover, we use aromatic N-containing ligands based on the following consideration: aromatic N-containing ligands not only may provide recognition sites for $\pi-\pi$ stacking interactions to form interesting supramolecular structures but also may have potential applications in fluorescent materials as model compounds for electroluminescence and optical-switching devices.[21]

On the basis of the aforementioned points, we successfully synthesized a series of new complexes constructed from inorganic molybdearsenate under mild hydrothermal synthesis conditions, namely, (4,4′-bipy)[Zn(4,4′-bipy)$_2$(H$_2$O)$_2$]$_2$-[(ZnO$_6$)(As$^{III}_3$O$_3$)$_2$Mo$_6$O$_{18}$]·7H$_2$O, **1**, [Zn(phen)$_2$(H$_2$O)]$_2$-[(ZnO$_6$)(As$^{III}_3$O$_3$)$_2$Mo$_6$O$_{18}$]·4H$_2$O, **2**, [Zn(2,2′-bipy)$_2$(H$_2$O)]$_2$-[(ZnO$_6$)(As$^{III}_3$O$_3$)$_2$Mo$_6$O$_{18}$]·4H$_2$O, **3**, [Zn(H4,4′-bipy)$_2$(H$_2$O)$_4$]-[(ZnO$_6$)(As$^{III}_3$O$_3$)$_2$Mo$_6$O$_{18}$]·8H$_2$O, **4**, (H$_2$4,4′-bipy)[Cu^{I}(4,4′-bipy)]$_2$[H$_2$As$^{V}_2$Mo$_6$O$_{26}$]·H$_2$O, **5**, (H$_2$4,4′-bipy)$_3$[As$^{V}_2$Mo$_6$O$_{26}$]·4H$_2$O **6**, (H$_2$4,4′-bipy)$_3$[As$^{V}_2$Mo$_6$O$_{26}$(H$_2$O)]·4H$_2$O, **7**, and (H$_2$4,4′-bipy)$_{2.5}$(H$_3$O)[As$^{V}_2$Mo$_6$O$_{26}$(H$_2$O)]·1.25H$_2$O, **8**. To the best of our knowledge, compounds **1**−**8** represent novel extended and modified structures based on the inorganic molybdearsenate clusters of [(ZnO$_6$)(As$_3$O$_3$)$_2$Mo$_6$O$_{18}$]$^{4-}$ and [H$_x$As$_2$Mo$_6$O$_{26}$]$^{(6-x)-}$. Moreover, compound **1** represents the first example of 3D supramolecular open framworks constructed from 2D metal−organic coordination polymer layers and molybdenum arsenate clusters of [(ZnO$_6$)(As$_3$O$_3$)$_2$-Mo$_6$O$_{18}$]$^{4-}$ with two types of channels. The unique structural character in **1** not only represents a new type of open-

(9) (a) Haber, J. *The Role of Molybdenum in Catalysis*; Climax Molybdenum: London, 1981. (b) Chen, C. C.;Wang, Q.; Lei, P. X.; Song, W. J.; Ma, W. H.; Zhao, J. C. *Environ. Sci. Technol.* **2006**, *40*, *3965*. (c) Kozhevnikov, I. V. *Chem. Rev.* **1998**, *98*, 171.

(10) (a) Dimitris, E.; Katsoulis. *Chem. Rev.* **1998**, *98*, 359. (b) Yamase, T. *Chem. Rev.* **1998**, *98*, 307. (c) Skupiski, W.; Malesa, M. *Appl. Catal.* **2002**, *236*, 223.

(11) (a) Haushalter, R. C.; Mundi, L. A. *Chem. Mater.* **1992**, *4*, 31. (b) Haushalter, R. C.; Strohmaier, K. G.; Lai, F. W. *Science.* **1989**, *246*, 1289. (c) Lighitfoot, P.; Masson, D. *Mater. Res. Bull.* **1995**, *30*, 1005. (d) Peloux, C. D.; Mialane, P.; Dolbecq, A.; Marrot, J.; Rivière, E.; Sécheresse, F. *J. Mater. Chem.* **2001**, *11*, 3392.

(12) (a) MacGiolla Coda, E.; Hodnett, B. K. In *New Developments in Selective Oxidation*; Centi, G., Trifirò, F., Eds.; Elsevier: Amsterdam, 1990; p 459. (b) Matsuura, I.; Kimura, N. In *New Developments in Selective Oxidation II*; Corberan Cortes, V., Vic Bellon, S., Eds.; Elsevier: Amsterdam, 1994; p 271.

(13) (a) Ramis, G.; Yi, L.; Busca, G.; DelArco, M.; Martin, C.; Rives, V.; Sanchez Escribano, V. *Mater. Chem. Phys.* **1998**, *55*, 173. (b) Daturi, M.; Busca, G.; Guesdon, A.; Borel, M. M. *J. Mater. Chem.* **2001**, *11*, 1726. (c) Hönicke, D.; Griesbaum, K.; Augenstein, R.; Yang, Y. *Chem. Ing. Tech.* **1987**, *59*, 222.

(14) (a) Kwak, W.; Rajkovic, L. M.; Pope, M. T.; Quicksall, C. O.; Matsumoto, K. Y.; Sasaki, Y. *J. Am. Chem. Soc.* **1977**, *99*, 6463. (b) Kwak, W.; Rajkovic, L. M.; Stalick, J. K.; Pope, M. T.; Quicksall, C. O. *Inorg. Chem.* **1976**, *15*, 2778. (c) Hsu, K. F.; Wang, S. L. *Inorg. Chem.* **1997**, *36*, 3049. (d) Hedman, B. *Acta. Crystallogr.* **1980,** *B36*, 2241.

(15) (a) Khan, M. I.; Chen, Q.; Zubieta, J. *Chem. Commun.* **1993**, 356. (b) Martin-Frère, J.; Jeannin, Y.; Robert, F.; Vaissermann, J. *Inorg. Chem.* **1991**, *30*, 3635. (c) He, Q. L.; Wang, E. B. *Inorg. Chim. Acta* **1999**, *295*, 244. (d) Fidalgo, E. G.; Neels, A.; Stoeckli-Evans, H.; Süss-Fink, G. *Polyhedron* **2002**, *21*, 1921.

(16) (a) Burkholder, E.; Wright, S.; Golub, V.; O'Connor, C. J.; Zubieta, J. *Inorg. Chem.* **2003**, *42*, 7460. (b) Burkholder, E.; Zubieta, J. *Inorg. Chim. Acta* **2004**, *357*, 301. (c) Chang, Y. D.; Zubieta, J. *Inorg. Chim. Acta* **1996**, *245*, 177.

(17) (a) Besecker, C. J.; Marritt, W. A. U.S. Patent 4900853 A, 1990; *Chem. Abstr.* **1990**, *113*, 134256. (b) Müller, A.; Peters, F.; Pope, M. T.; Gatteschi, D. *Chem. Rev.* **1998**, *98*, 239. (c) Mizuno, N.; Misono, M. *Chem. Rev.* **1998**, *98*, 199. (d) He, Q. L.; Wang, E. B.; Hu, C. W.; Xu, L. *J. Mol. Struct.* **1999**, *484*, 139. (e) Fruchart, J. M.; Herve, G.; Launay, J. P.; Massart, R. *J. Inorg. Nucl. Chem.* **1976**, *38*, 1627.

(18) (a) Flem, G. L. *Eur. J. Solid State Inorg. Chem.* **1991**, *28*, *3*. (b) Bu, X. H.; Gier, T. E.; Stucky, G. D. *Chem. Commun.* **1997**, 2271. (c) Wiggin, S. B.; Weller, M. T. *Chem. Commun.* **2006**, 1100.

(19) (a) Johnson, C. D.; Skakle, J. M. S.; Johnston, M. G.; Feldmann, J.; Macphee, D. E. *J. Mater. Chem.* ***2003***, *13*, 1429. (b) Johnson, C. D.; Feldmann, J.; Macphee, D. E.; Worrall, F.; Skakleb, J. M. S. *Dalton Trans.* **2004**, 3611. (c) Robins, R. *Metal Trans. B* **1981**, *12*, 103. (d) Papassiopi, N.; Stefanakis, M.; Kontopoulos, A. *Hydrometallurgy* **1996**, *41*, 243.

(20) (a) Hagrman, P. J.; Hagrman, D.; Zubieta, J. *Angew. Chem., Int. Ed.* **1999**, *38*, 2638. (b) Hagrman, P. J.; Finn, R. C.; Zubieta, J. *J. Solid State Chem.* **2001**, *3*, 745. (c) Khan, M. I.; Yohannes, E.; Doedens, R. J. *Angew. Chem., Int. Ed.* **1999**, *111*, 1374. (d) Xiao, D. R.; Wang, E. B.; An, H. Y.; Su, Z. M.; Li, Y. G.; Gao, L.; Sun, C. Y.; Xu, L. *Chem.—Eur. J.* **2005**, *11*, 6673.

(21) (a) Peng, Z. H. *Angew. Chem., Int. Ed.* **2004**, *43*, 930. (b) Grummt, U. W.; Birckner, E.; Klemm, E.; Egbe, D. A. M.; Heise, B. *J. Phys. Org. Chem.* **2000**, *13*, 112.

framework structures but also indicates that Mo−As−O clusters can be effectively used as functional second building units (SBUs) to construct novel open-framework functionalized materials.

Experimental Section

General Considerations. All chemicals were commercially purchased and used without further purification. Elemental analyses (C, H, and N) were performed on a Perkin-Elmer 2400 CHN elemental analyzer; As, Mo, Zn, and Cu were analyzed on a PLASMA-SPEC(I) ICP atomic emission spectrometer. XPS analyses were performed on a VG ESCALABMKII spectrometer with a Mg Kα (1253.6 eV) achromatic X-ray source. The vacuum inside the analysis chamber was maintained at 6.2×10^{-6} Pa during the analysis. IR spectra were recorded in the range of 400−4000 cm^{-1} on an Alpha Centaurt FT/IR Spectrophotometer using KBr pellets. TG analyses were performed on a Perkin-Elmer TGA7 instrument in flowing N_2 with a heating rate of 10 °C·min^{-1}. Excitation and emission spectra were obtained on a SPEX FL-2T2 spectrofluorometer equipped with a 450 W xenon lamp as the excitation source.

Synthesis. (4,4′-bipy)[Zn(4,4′-bipy)$_2$(H$_2$O)$_2$]$_2$[(ZnO$_6$)(As$^{III}_3$O$_3$)$_2$Mo$_6$O$_{18}$]·7H$_2$O (1). A mixture of $Zn(OAc)_2$·$2H_2O$ (0.5 mmol), $NaAsO_2$ (1 mmol), Na_2MoO_4·$2H_2O$ (1 mmol), 4,4′-bipy (0.5 mmol), and water (8 mL) was stirred for 30 min in air; then the pH value of the mixture was carefully adjusted to about 6.84, and it was sealed in an 18 mL Teflon-lined autoclave, which was heated at 140 °C for 96 h. After the mixture was slowly cooled to room temperature, colorless block crystals of **1** were filtered off, washed with distilled water, and dried at ambient temperature (30% yield based on Zn). Anal. Calcd for (4,4′-bipy)[Zn(4,4′-bipy)$_2$(H$_2$O)$_2$]$_2$-[(ZnO$_6$)(As$^{III}_3$O$_3$)$_2$Mo$_6$O$_{18}$]·7H$_2$O: C, 22.40; H, 2.33; As, 16.77; Mo, 21.48; N, 5.23, Zn, 7.32%. Found: C, 22.58; H, 2.13; As, 16.62; Mo, 21.66; N, 5.36; Zn, 7.18%. FT-IR data (cm^{-1}): 3334 (w), 1619 (m), 1539 (m), 1494(w), 1417 (m), 1226 (m), 1211 (w), 1072 (w), 1049 (w), 944 (s), 887 (s), 813 (s), 779 (s), 744 (s), 654 (s), 642 (m), 613 (w), 565 (w), 522 (w), 462 (w), 455 (w), 433 (w).

[Zn(phen)$_2$(H$_2$O)]$_2$[(ZnO$_6$)(As$^{III}_3$O$_3$)$_2$Mo$_6$O$_{18}$]·4H$_2$O (2). A mixture of $Zn(OAc)_2$·$2H_2O$ (0.5 mmol), $NaAsO_2$ (1 mmol), Na_2MoO_4·$2H_2O$ (1 mmol), phen (0.5 mmol), and water (8 mL) was stirred for 30 min in air; then the pH value of the mixture was carefully adjusted to about 6.54, and it was sealed in an 18 mL Teflon-lined autoclave, which was heated at 140 °C for 96 h. After the mixture was slowly cooled to room temperature, colorless block crystals of **2** were filtered off, washed with distilled water, and dried at ambient temperature (56% yield based on Zn). Anal. Calcd for [Zn-(phen)$_2$(H$_2$O)]$_2$[(ZnO$_6$)(As$^{III}_3$O$_3$)$_2$Mo$_6$O$_{18}$]·4H$_2$O: C, 22.78; H, 1.75; As, 17.77; Mo, 22.75; N, 4.43; Zn, 7.75%. Found: C, 22.62; H, 1.54; As, 17.80; Mo, 22.93; N, 4.26; Zn, 7.93%. FT-IR data (cm^{-1}): 3370 (w), 3274 (w), 1625 (w), 1605 (w), 1581 (m), 1518 (m), 1495 (w), 1454 (w), 1427 (s), 1341 (w), 1319 (w), 1307 (w), 1223 (w), 1210 (w), 1149 (w), 1103 (w), 1054 (w), 935 (s), 905 (s), 887 (s), 866 (m), 850 (s), 814 (s), 798 (s), 725 (s), 671 (s), 611 (m), 605 (m), 572 (w), 526 (w), 463 (w), 426 (w), 410 (w).

[Zn(2,2′-bipy)$_2$(H$_2$O)]$_2$[(ZnO$_6$)(As$^{III}_3$O$_3$)$_2$Mo$_6$O$_{18}$]·4H$_2$O (3). The preparation of **3** was similar to that of **2** except that 2,2′-bipy was used instead of phen. The pH value of the mixture was 6.68. Colorless block crystals of **3** were obtained in a 50% yield based on Zn. Anal. Calcd for [Zn(2,2′-bipy)$_2$(H$_2$O)]$_2$[(ZnO$_6$)(As$^{III}_3$O$_3$)$_2$-Mo$_6$O$_{18}$]·4H$_2$O: C, 19.74; H, 1.82; As, 18.47; Mo, 23.65; N, 4.60; Zn, 8.06%. Found: C, 19.56; H, 1.66; As, 18.62; Mo, 23.75; N, 4.42; Zn, 8.21%. FT-IR data (cm^{-1}): 3429 (m), 3075 (w), 1627 (w), 1604 (m), 1596 (s), 1576 (w), 1567 (w), 1490 (m), 1474 (m), 1442 (s), 1317 (w), 1284 (w), 1248 (w), 1175 (w), 1160 (w), 1121 (w), 1104 (w), 1064 (w), 1047 (w), 1023 (m), 1013 (w), 933 (s), 902 (s), 874 (s), 808 (s), 778 (m), 737 (m), 678 (s), 650 (s), 611 (m), 565 (m), 520 (w), 465 (w), 426 (w), 413 (w).

[Zn(H4,4′-bipy)$_2$(H$_2$O)$_4$][(ZnO$_6$)(As$^{III}_3$O$_3$)$_2$Mo$_6$O$_{18}$]·8H$_2$O (4). A mixture of $Zn(OAc)_2$·$2H_2O$ (0.5 mmol), $NaAsO_2$ (1 mmol), Na_2MoO_4·$2H_2O$ (1 mmol), 4,4′-bipy (0.5 mmol), and water (8 mL) was stirred for 30 min in air; then the pH value of the mixture was carefully adjusted to about 5.20, and it was sealed in an 18 mL Teflon-lined autoclave, which was heated at 140 °C for 96 h. After the mixture was slowly cooled to room temperature, colorless platelet crystals of **4** were filtered off, washed with distilled water, and dried at ambient temperature (36% yield based on Zn). Anal. Calcd for [Zn(H4,4′-bipy)$_2$(H$_2$O)$_4$][(ZnO$_6$)(As$^{III}_3$O$_3$)$_2$Mo$_6$O$_{18}$]·8H$_2$O: C, 11.09; H, 1.95; As, 20.75; Mo, 26.57; N, 2.59; Zn, 6.04%. Found: C, 12.11; H, 1.78; As, 21.85; Mo, 26.74; N, 2.46; Zn, 5.92%. FT-IR data (cm^{-1}): 3447 (m), 1642 (w), 1613 (s), 1540 (w), 1494 (w), 1417 (m), 1375 (w), 1337 (w), 1227 (m), 1073 (w), 1048 (w), 1029 (w), 1012 (w), 951 (m), 933 (m), 890 (s), 863 (s), 841 (m), 815 (s), 781 (m), 734 (s), 676 (m), 641 (m), 613 (w), 565 (w), 523 (w), 458 (w), 435 (w).

(H$_2$4,4′-bipy)[Cu^{I}(4,4′-bipy)]$_2$[H$_2$As$^{V}_2$Mo$_6$O$_{26}$]·H$_2$O (5). A mixture of $CuCl_2$·$2H_2O$ (0.5 mmol), $NaAsO_2$ (1 mmol), Na_2MoO_4·$2H_2O$ (1 mmol), 4,4′-bipy (0.5 mmol), and water (8 mL) was stirred for 30 min in air; then the pH value of the mixture was carefully adjusted to about 5.40, and it was sealed in an 18 mL Teflon-lined autoclave, which was heated at 130 °C for 96 h. After the mixture was slowly cooled to room temperature, red block crystals of **5** were filtered off, washed with distilled water, and dried at ambient temperature (67% yield based on Cu). Anal. Calcd for (H$_2$4,4′-bipy)[Cu^{I}(4,4′-bipy)]$_2$[H$_2$As$^{V}_2$Mo$_6$O$_{26}$]·H$_2$O: C, 20.48; H, 1.72; As, 8.52; Mo, 32.72; N, 4.78; Cu, 7.23%. Found: C, 20.61; H, 1.56; As, 8.42; Mo, 32.54; N, 4.96; Cu, 7.42%. FT-IR data (cm^{-1}): 3419 (m), 3095 (w), 1612 (s), 1532 (w), 1488 (m), 1417 (m), 1375 (w), 1327 (w), 1221 (w), 1202 (w), 1072 (w), 948 (m), 897 (s), 864 (m), 811 (s), 762 (m), 665 (s), 583 (w), 517 (w), 469 (w), 419 (w).

(H$_2$4,4′-bipy)$_3$[As$^{V}_2$Mo$_6$O$_{26}$]·4H$_2$O (6). A mixture of $Cd(OAc)_2$·$2H_2O$ (0.5 mmol), $NaAsO_2$ (1 mmol), Na_2MoO_4·$2H_2O$ (1 mmol), 4,4′-bipy (0.5 mmol), and water (8 mL) was stirred for 30 min in air; then the pH value of the mixture was carefully adjusted to about 3.25, and it was sealed in an 18 mL Teflon-lined autoclave, which was heated at 130 °C for 96 h. After the mixture was slowly cooled to room temperature, colorless block crystals of **6** were filtered off, washed with distilled water, and dried at ambient temperature (56% yield based on Mo). Anal. Calcd for (H$_2$4,4′-bipy)$_3$[As$^{V}_2$Mo$_6$O$_{26}$]·4H$_2$O: C, 21.34; H, 2.27; As, 8.88; Mo, 34.10; N, 4.98%. Found: C, 21.46; H, 2.43; As, 8.76; Mo, 33.96; N, 5.12%. FT-IR data (cm^{-1}): 3524 (w), 3456 (m), 3115 (w), 3086 (w), 3064 (w), 1635 (m), 1625 (m), 1611 (s), 1601 (s), 1590 (s), 1487 (m), 1476 (m), 1416 (w), 1369 (w), 1341 (w), 1298 (w), 1233 (w), 1218 (w), 1200 (w), 1124 (w), 1105 (w), 1066 (w), 1029 (w), 1004 (w), 942 (m), 895 (s), 873 (m), 840 (m), 796 (s), 680 (s), 666 (s), 630 (m), 587 (m), 565 (w), 526 (w), 460 (w), 407 (w).

(H$_2$4,4′-bipy)$_3$[As$^{V}_2$Mo$_6$O$_{26}$(H$_2$O)]·4H$_2$O (7) and (H$_2$4,4′-bipy)$_{2.5}$(H$_3$O)[As$^{V}_2$Mo$_6$O$_{26}$(H$_2$O)]·1.25H$_2$O (8). The preparations of **7** and **8** were similar to that of **6** except that $Zn(OAc)_2$·$2H_2O$ and $ZnCl_2$·$2H_2O$ were used instead of $Cd(OAc)_2$·$2H_2O$. The pH value of the mixture was 3.46 for **7** and 3.42 for **8.** Colorless crystals of **7** were obtained in a 65% yield based on Mo. Anal. Calcd for (H$_2$4,4′-bipy)$_3$[As$^{V}_2$Mo$_6$O$_{26}$(H$_2$O)]·4H$_2$O: C, 21.12; H, 2.36; As, 8.78; Mo, 33.74; N, 4.93%. Found: C, 21.27; H, 2.52; As, 8.51; Mo, 33.53; N, 4.78%. FT-IR data (cm^{-1}): 3527 (w), 3457 (m), 3116 (w), 3087 (w), 3065 (w), 1635 (m), 1625 (m), 1612 (s), 1601

Table 1. Crystal Data and Structure Refinement for **1**−**8**

	1	**2**	**3**	**4**
formula	$C_{50}H_{62}As_6Mo_6N_{10}O_4Zn_3$	$C_{48}H_{44}As_6Mo_6N_8O_{36}Zn_3$	$C_{40}H_{44}As_6Mo_6N_8O_{36}Zn_3$	$C_{20}H_{42}As_6Mo_6N_4O_{42}Zn_2$
formula weight	2680.37	2530.18	1546.95	2166.48
T (K)	293(2)	293(2)	293(2)	293(2)
λ (Å)	0.71073	0.71073	0.71073	0.71073
cryst syst	monoclinic	triclinic	monoclinic	triclinic
space group	$P2/n$	$P\bar{1}$	$P2/n$	$P\bar{1}$
a (Å)	18.349(4)	10.493(2)	18.117(4)	9.3252(2)
b (Å)	11.471(2)	10.781(2)	9.3968(2)	12.051(2)
c (Å)	22.932(5)	15.639(3)	19.658(4)	14.174(3)
α (deg)	90	77.55(3)	90	114.93(3)
β (deg)	92.26(3)	77.86(3)	94.08(3)	93.63(3)
γ (deg)	90	78.81(3)	90	105.82(3)
V (Å^3)	4823.0(2)	1668.3(6)	3338.2(1)	1360.4(5)
Z	2	1	2	1
μ (mm^{-1})	3.609	5.203	5.195	5.935
R_1[a] [$I > 2\sigma(I)$]	0.0531	0.0580	0.0500	0.0783
wR_2[b] [$I > 2\sigma(I)$]	0.0820	0.1149	0.1376	0.1672

	5	**6**	**7**	**8**
formula	$C_{30}H_{30}As_2Cu_2Mo_6N_6O_{27}$	$C_{30}H_{38}As_2Mo_6N_6O_{30}$	$C_{30}H_{40}As_2Mo_6N_6O_{31}$	$C_{25}H_{32.5}As_2Mo_6N_5O_{29.25}$
formula weight	1759.16	1688.14	1706.16	1596.54
T (K)	293(2)	293(2)	293(2)	293(2)
λ (Å)	0.71073	0.71073	0.71073	0.71073
cryst syst	triclinic	monoclinic	monoclinic	triclinic
space group	$P\bar{1}$	$C2/m$	$P2_1/n$	$P\bar{1}$
a (Å)	10.852(2)	14.691(3)	11.795(2)	11.225(2)
b (Å)	11.389(2	18.645(4)	24.301(5)	14.065(3)
c (Å)	11.976(2)	10.623(2)	17.028(3)	15.201(3)
α (deg)	66.89(3)	90	90.00	100.15(3)
β (deg)	84.75(3)	127.52(3)	94.64(3)	93.02(3)
γ (deg)	64.78(3)	90	90.00	111.94(3)
V (Å^3)	1226.5(4)	2307.9(8)	4864.9(2)	2172.9(7)
Z	1	2	4	2
μ(mm^{-1})	3.763	3.111	2.955	3.295
R_1[a] [$I > 2\sigma(I)$]	0.0787	0.0247	0.0389	0.0468
wR_2[b] [$I > 2\sigma(I)$]	0.1940	0.0538	0.0955	0.1005

[a] $R_1 = \sum||F_0| - |F_C||/\sum|F_0|$. [b] $wR_2 = \sum[w(F_0^2 - F_C^2)^2]/\sum[w(F_0^2)^2]^{1/2}$.

(s), 1591 (s), 1448 (m), 1476 (m), 1416 (w), 1369 (w), 1341 (w), 1229 (w), 1233 (w), 1218 (w), 1201 (w), 1124 (w), 1106 (w), 1067 (w), 1028 (w), 1004 (w), 942 (m), 896 (s), 873 (m), 840 (m), 798 (s), 681 (s), 666 (s), 630 (m), 588 (m), 565 (w), 527 (w), 461 (w), 408 (w). Colorless block crystals of **8** were obtained in a 50% yield based on Mo. Anal. Calcd for $(H_2$4,4′-bipy$)_{2.5}(H_3O)[As^V_2Mo_6O_{26}(H_2O)]\cdot 1.25H_2O$: C, 18.81; H, 2.05; As, 9.39; Mo, 36.06; N, 4.39%. Found: C, 18.92; H, 2.18; As, 9.19; Mo, 35.92; N, 4.53%. FT-IR data (cm^{-1}): 3522 (w), 3452 (m), 3114 (w), 3086 (w), 3064 (w), 1634 (m), 1625 (m), 1611 (s), 1601 (s), 1592 (s), 1449 (m), 1479 (m), 1417 (w), 1369 (w), 1342 (w), 1229 (w), 1233 (w), 1217 (w), 1201 (w), 1124 (w), 1106 (w), 1067 (w), 1029 (w), 1005 (w), 942 (m), 895 (s), 872 (m), 840 (m), 797 (s), 680 (s), 666 (s), 630 (m), 587 (m), 565 (w), 528 (w), 463 (w), 410 (w).

X-ray Crystallography. Intensity data were collected on a Rigaku R-AXIS RAPID IP diffractometer with Mo Kα monochromated radiation (λ = 0.71073 Å) at 293 K. Empirical absorption correction was applied. The structures of **1**−**8** were solved by the direct method and refined by the Full-matrix least-squares on F^2 using the SHELXTL-97 software.[22] All of the non-hydrogen atoms were refined anisotropically. The organic hydrogen atoms were generated geometrically, except for the hydrogen atoms attached to OW1 in compound **7**, which were located from difference maps; those attached to other water molecules were not located.

(22) (a) Sheldrick, G. M. *SHELXL 97, Program for Crystal Structure Refinement*; University of Göttingen: Göttingen, Germany, 1997. (b) Sheldrick, G. M. *SHELXL 97, Program for Crystal Structure Solution*; University of Göttingen: Göttingen, Germany, 1997.

A summary of crystal data and structure refinement for compounds **1**−**8** is provided in Table 1. Selected bond lengths and angles of **1**−**8** with standard deviations in parentheses are listed in Table 2.

The CCDC reference numbers are 606917 for **1**, 600759 for **2**, 606872 for **3**, 606916 for **4**, 610482 for **5**, 602072 for **6**, 602551 for **7**, and 606871 for **8**.

Results and Discussion

Syntheses. In our case, the pH value of a solution is an importent factor for the formation of extended structure of molybdenum arsenate. At lower pH values, the N-ligand groups tend to be protonated and fail to bond to the metal ions. We have done a lot of control experiments, and we finally obtained compounds of **1**−**8**.

Crystal structures of 1−**4.** The structure of $[(CoO_6)(As_3O_3)_2Mo_6O_{18}]^{4-}$ was characterized in the compound $[Co(en)_3H_3O][(CoO_6)(As_3O_3)_2Mo_6O_{18}]^{4-}$ through single-crystal X-ray diffraction by our groups in 1999.[15c] Its structure is composed of the well-known A-type Anderson structure capped with two cyclic As_3O_6 trimers on opposite faces. However, it is unexploited that the polyoxoanions $[(MO_6)(As_3O_3)_2Mo_6O_{18}]^{4-}$ (M = metal) have been used as inorganic building blocks to construct extended and modified structures. Herein, we successfully synthesized compounds of **1**−**4** constructed from polyanions $[(ZnO_6)(As_3O_3)_2$-

Table 2. Bond Lengths (Å) and Angles (deg) with Standard Deviations in Parentheses of Compounds **1**−**8**[a]

compound **1**

Zn(1)−O(1)	2.067(5)	Zn(3)−N(6)	2.189(1)	As(1)−O(2)	1.753(6)	As(3)−O(1)	1.774(5)
Zn(1)−O(2)	2.096(6)	Zn(3)−N(5)	2.255(9)	As(1)−O(6)	1.786(6)	As(3)−O(8)	1.783(7)
Zn(2)−OW1	2.078(6)	Mo(1)−O(9)	1.689(6)	As(2)−O(6)	1.754(6)	Mo(2)−O(1)	2.322(6)
Zn(3)−OW2	2.123(5)	Mo(3)−O(5)	1.938(6)	As(2)−O(7)#1	1.772(6)		

O(4)−Mo(1)−O(1)	70.1(2)	O(2)−As(1)−O(8)#1	102.2(3)	O(3)−Zn(1)−O(2)#1	86.4(2)	N(1)−Zn(2)−N(2)	180.000(1)
O(11)−Mo(2)−O(3)	163.3(3)	O(6)−As(2)−O(7)#1	98.1(3)	O(3)−Zn(1)−O(3)#1	180.0(3)	OW2−Zn(3)−N(5)	88.78(9)
O(15)−Mo(3)−O(13)	100.1(3)	O(1)−As(3)−O(7)	99.6(2)	OW1−Zn(2)−N(1)	87.48(1)	N(6)−Zn(3)−N(5)	180.000(2)

compound **2**

Zn(1)−O(2)	2.062(6)	Zn(2)−N(3)	2.146(9)	As(1)−O(3)	1.779(6)	As(3)−O(6)	1.796(7)
Zn(1)−O(3)	2.090(6)	Zn(2)−N(4)	2.201(9)	As(1)−O(8)	1.785(8)	As(3)−O(8)	1.798(8)
Zn(2)−O(1)	2.137(7)	Mo(1)−O(14)	1.695(8)	As(2)−O(2)	1.792(6)	Mo(2)−O(5)	1.942(6)
Zn(2)−OW1	2.114(8)	Mo(3)−O(2)	2.319(7)	As(2)−O(7)	1.789(7)		

O(14)−Mo(1)−O(11)#1	97.1(4)	O(7)#1−As(1)−O(8)	100.5(4)	O(2)#1−Zn(1)−O(2)	180.0(3)	N(3)−Zn(2)−N(2)	166.8(4)
O(4)−Mo(2)−O(3)	70.7(3)	O(9)#1−As(2)−O(7)	99.5(3)	N(3)−Zn(2)−N(4)	77.0(3)	O(9)−As(3)−O(8)	97.8(3)
O(10)−Mo(3)−O(2)	165.0(3)	O(2)−Zn(1)−O(6)	85.8(2)				

compound **3**

Zn(1)−O(7)	2.077(5)	Zn(2)−N(4)	2.082(7)	As(1)−O(4)	1.768(5)	As(3)−O(5)	1.786(5)
Zn(1)−O(3)	2.097(4)	Zn(2)−N(3)	2.184(7)	As(1)−O(2)	1.791(5)	As(3)−O(3)	1.794(5)
Zn(2)−O(1)	2.179(5)	Mo(1)−O(11)	1.713(5)	As(2)−O(5)	1.777(5)	Mo(2)−O(8)	1.949(5)
Zn(2)−OW1	2.151(6)	Mo(3)−O(3)	2.313(5)	As(2)−O(7)	1.798(5)		

O(1)−Mo(1)−O(2)	165.8(2)	O(6)−As(1)−O(2)	100.3(2)	O(7)#1−Zn(1)−O(7)	180.0(4)	O(1)−Zn(2)−N(3)	172.2(2)
O(8)−Mo(2)−O(2)	71.30(2)	O(5)−As(2)−O(7)	99.4(2)	N(4)−Zn(2)−N(3)	76.9(2)	O(6)−As(3)−O(3)	98.8(2)
O(15)−Mo(3)−O(9)	102.3(2)	O(7)#1−Zn(1)−O(2)	86.09(2)				

compound **4**

Zn(1)−O(1)	2.072(9)	Zn(2)−N(1)	2.144(1)	As(1)−O(5)	1.805(1)	As(3)−O(4)	1.785(1)
Zn(1)−O(2)	2.115(1)	Mo(1)−O(9)	1.699(1)	As(2)−O(5)	1.773(1)	As(3)−O(6)	1.802(1)
Zn(2)−OW1	2.091(2)	Mo(3)−O(3)#1	2.329(1)	As(2)−O(6)	1.797(1)	Mo(2)−O(8)	1.925(1)
Zn(2)−OW2	2.068(2)	As(1)−O(4)	1.790(1)				

O(14)#1−Mo(1)−O(2)#1	70.8(3)	O(4)−As(1)−O(5)	100.6(4)	O(3)#1−Zn(1)−O(3)	180.0(6)	N(1)#2−Zn(2)−N(1)	180.000(1)
O(12)−Mo(2)−O(3)#1	91.0(4)	O(5)−As(2)−O(3)	98.0(4)	OW1#2−Zn(2)−N(1)	88.7(6)	O(4)−As(3)−O(2)	99.7(4)
O(15)−Mo(3)−O(3)#1	164.8(4)	O(3)#1−Zn(1)−O(2)	85.8(3)				

compound **5**

Cu(1)−N(2)#1	1.920(1)	Mo(1)−O(7)	1.681(1)	As(1)−O(2)	1.622(1)	As(1)−O(12)	1.685(9)
Cu(1)−N(1)	1.926(1)	Mo(2)−O(3)	1.901(1)	As(1)−O(1)	1.674(1)	As(1)−O(13)	1.723(1)
Cu(1)−O(9)	2.475(5)	Mo(3)−O(2)#2	2.419(1)				

O(3)−Mo(1)−O(13)#2	73.5(4)	N(2)#1−Cu(1)−N(1)	160.5(7)	O(2)−As(1)−O(1)	113.4(5)	O(10)−Mo(3)−O(4)	98.2(5)
O(8)−Mo(2)−O(1)	166.2(5)	O(2)−As(1)−O(12)	105.2(6)				

compound **6**

Mo(1)−O(1)	1.711(2)	Mo(2)−O(3)	1.708(2)	As(1)−O(8)	1.692(2)	As(1)−O(6)#2	1.6959(2)
Mo(1)−O(7)	1.901(2)	Mo(2)−O(8)	2.375(2)	As(1)−O(6)#1	1.6959(2)		

O(1)#1−Mo(1)−O(6)	164.44(9)	O(4)−Mo(2)−O(8)	74.16(8)	O(6)#1−As(1)−O(5)	107.17(8)	O(8)−As(1)−O(6)#2	111.82(8)

compound **7**

As(1)−O(19)	1.669(3)	As(1)−O(26)	1.713(3)	As(2)−O(25)	1.689(3)	As(2)−O(20)	1.686(3)
As(1)−O(23)	1.670(3)	Mo(6)−O(22)	2.321(3)	As(2)−O(22)	1.686(3)	Mo(5)−OW1	2.296(3)
As(1)−O(24)	1.689(3)	As(2)−O(21)	1.670(3)				

O(13)−Mo(1)−O(24)	70.34(1)	O(7)−Mo(4)−OW1	160.06(2)	O(19)−As(1)−O(24)	115.72(2)	O(21)−As(2)−O(20)	112.55(1)
O(3)−Mo(2)−O(20)	167.41(2)	OW1−Mo(5)−O(21)	70.39(1)	O(21)−As(2)−O(25)	106.29(2)	O(11)−Mo(6)−O(12)	103.09(2)
O(6)−Mo(3)−O(15)	99.75(2)	O(24)−As(1)−O(26)	104.76(2)				

compound **8**

As(1)−O(5)	1.607(1)	As(1)−O(7)	1.710(1)	As(2)−O(1)	1.663(5)	As(2)−O(26)	1.694(5)
As(1)−O(22)	1.696(5)	Mo(1)−O(2)	1.681(8)	As(2)−O(20)	1.685(5)	Mo(2)−OW1	2.468(7)
As(1)−O(11)	1.700(5)	Mo(6)−O(20)	2.290(5)	As(2)−O(15)	1.686(5)		

O(4)−Mo(1)−O(15)	70.3(2)	O(24)−Mo(3)−O(7)	168.2(4)	O(5)−As(1)−O(11)	117.3(7)	O(19)−Mo(5)−O(26)	88.5(3)
O(15)−Mo(2)−OW1	68.2(2)	O(9)−Mo(4)−O(23)	100.4(3)	O(1)−As(2)−O(15)	108.5(3)	O(16)−Mo(6)−O(5)	95.0(5)
O(6)−Mo(2)−OW1	165.6(3)	O(11)−As(1)−O(7)	97.0(7)	O(1)−As(2)−O(26)	111.1(3)		

[a] Symmetry transformations used to generate equivalent atoms: (**1**) #1 $-x+1,-y+1,-z$; #2 $-x+3/2, y, -z-1/2$; #3 $-x+3/2, y, -z+1/2$; #4 $x, y+1, z$; #5 $x, y-1, z$; #6 $-x+3/2, y-1, -z-1/2$; #7 $-x+3/2, y-1, -z+1/2$; #8 $-x+1, -y+2, -z$; (**2**) #1 $-x, -y, -z$; (**3**) #1 $-x-1, -y+1, -z$; #2 $-x-3/2, y, -z+1/2$; (**4**) #1 $-x, -y, -z$; #2 $-x+1, -y, -z+1$; (**5**) #1 $-x, -y, -z$; #2 $-x-1, -y, -z$; (**6**) #1 $-x+1, y, -z+3$; #2 $-x+1, -y, -z+3$; #3 $x, -y, z$; #4 $-x, y, -z+2$; #5 $-x, -y, -z+1$; (**8**) #1 $-x+1, -y+1, -z$.

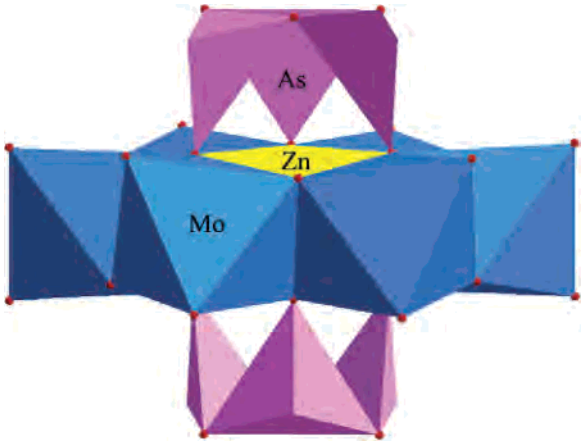

Figure 1. Representation of $[(ZnO_6)(As_3O_3)_2Mo_6O_{18}]^{4-}$ building block showing the metal atoms and their coordination polyhedra.

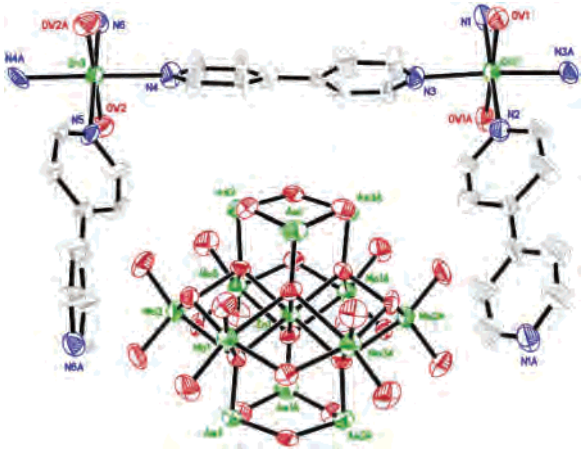

Figure 2. ORTEP drawing of **1** with thermal ellipsoids at 50% probability. The lattice water molecules and free 4,4′-bipy molecules have been omitted for clarity.

$Mo_6O_{18}]^{4-}$ (Figure 1) by a hydrothermal technique. The $[(ZnO_6)(As_3O_3)_2Mo_6O_{18}]^{4-}$ cluster is derived from the A-type Anderson anion $[(ZnO_6)Mo_6O_{18}]^{10-}$, in which a central {ZnO6} octahedron is coordinated with six {MoO6} octahedra hexagonally arranged by sharing their edges in a plane. The cyclic As_3O_6 trimers are capped on opposite faces of Anderson-type anion plane. Each As_3O_6 group consists of three AsO_3 pyramids linked in a triangular arrangement by sharing corners and bonded to the central ZnO_6 octahedron and two MoO_6 octahedra via μ_3-oxo groups. Compounds **1**−**4** contain the same polyanion $[(ZnO_6)(As_3O_3)_2$-$Mo_6O_{18}]^{4-}$, so we only described the bond lengths and angles of the polyanion $[(ZnO_6)(As_3O_3)_2Mo_6O_{18}]^{4-}$ in compound **1**.

Single-crystal X-ray structural analysis shows that compound **1** is constructed from the 2D square gridlike sheets $[Zn(4,4'\text{-bipy})_2(H_2O)_2]^{2+}$, linked by polyanions $[(ZnO_6)$-$(As_3O_3)_2Mo_6O_{18}]^{4-}$ via hydrogen-bonding to form a 3D supramolecular framework with two types of channels, and the "guest" 4,4′-bipy ligands and water molecules reside in the channels. Compound **1** is made up of $[(ZnO_6)(As_3O_3)_2$-$Mo_6O_{18}]^{4-}$ clusters, zinc-4,4′-bipy coordination complexes, free 4,4′-bipy molecules, and lattice water molecules (Figure 2). Three kinds of oxygen atoms exist in the cluster according to the way the oxygen atoms coordinated: terminal oxygen

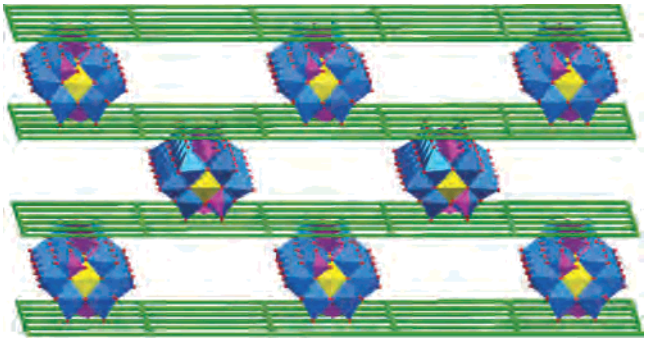

Figure 3. Schematic illustration of the 3D supramolecular framework of **1** constructed from 2D square gridlike layers and $[(ZnO_6)(As_3O_3)_2Mo_6O_{18}]^{4-}$ clusters.

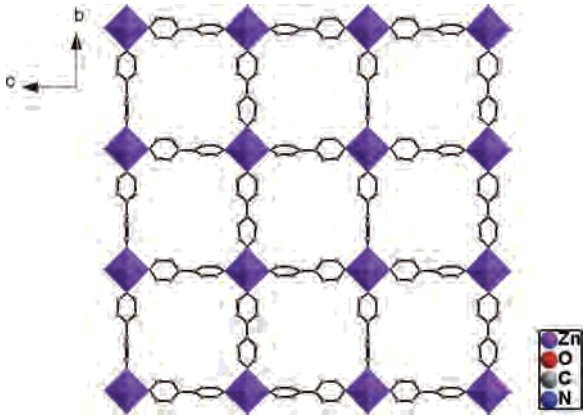

Figure 4. Polyhedral representation of the 2D square gridlike sheets in **1** showing square cavities with dimensions of 11.466 × 11.466 Å running along the *a* axis.

O_t, double-bridging oxygen $O(\mu_2)$, and four-bridging oxygen $O(\mu_4)$. Thus, the Mo−O bond lengths fall into three classes: $Mo-O_t$ = 1.665 (7)−1.731(5) Å, $Mo-O(\mu_2)$ = 1.888(7)−1.929(5) Å, and $Mo-O(\mu_4)$ = 2.313(5)−2.343(6) Å. And the As−O bond lengths fall into two classes: $As-O(\mu_2)$ = 1.764(5)−1.790(7) Å and $As-O(\mu_4)$ 1.763(5)−1.773(5) Å. The central Zn(1)−O distances vary from 2.063(5) to 2.089-(6) Å, indicating that the $\{ZnO_6\}$ octahedron is slightly distorted. The O−Zn(1)−O angles are in the range of 86.2-(2)−180.0(3)°.

There are other two crystallization-independent zinc atoms in **1**. Both Zn(2) and Zn(3) are coordinated by four nitrogen donors from four 4,4′-bipy ligands (Zn(2)−N = 2.211(8), 2.215(8), 2.243(8) Å and Zn(3)−N = 2.189(8), 2.197(8), 2.252(8) Å) and two water molecules ($(Zn(2)-OW_2$ = 2.085-(6) Å and $Zn(3)-OW_2$ = 2.123(5) Å) to furnish distorted octahedron geometry. Each zinc atom acts as a 4-connected node coordinated with four 4,4′-bipy groups to generate a two-dimensional square gridlike coordination framework of (4,4) topology (Figures 4and S1). Each layer shows square cavities with dimensions of 11.466 × 11.466 Å. (based on $d_{Zn\cdots Zn}$). Moreover, it is noteworthy that the layers are perfectly planar with the equatorial plane of the zinc coordination sphere. The $\{Zn(4,4'\text{-bipy})_2\}_n^{2n+}$ layers lie parallel to the *bc* plane, and adjacent square-grid layers are further linked by $[(ZnO_6)(As_3O_3)_2Mo_6O_{18}]^{4-}$ clusters via hydrogen bonding to form a three-dimensional supramolecular framework with 1D channels (Figures 3 and S2). This

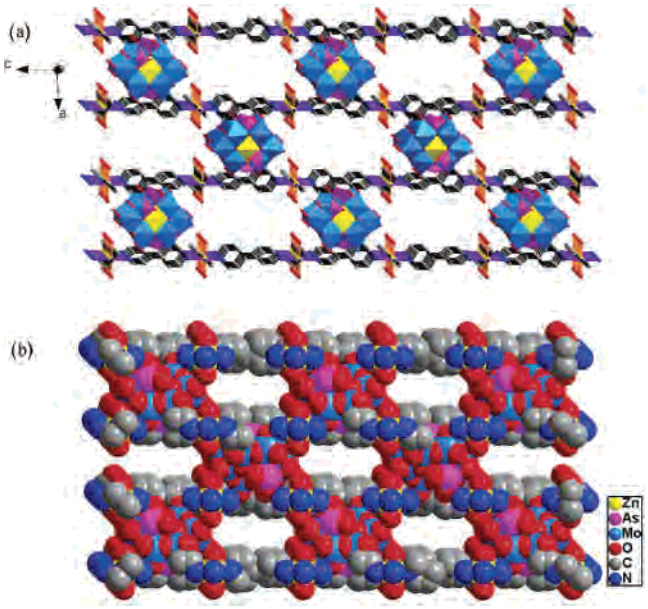

Figure 5. (a) Polyhedral and ball-stick representation of the 3D supramolecular framework structure of **1** along the *b* axis. (b) Space-filling diagram of the 3D supramolecular channel framework of **1** along the *b* axis. Lattice water molecules and free organic molecules have been omitted for clarity.

organization leads to the formation of channels in two directions: along the *b* axis, rectangular channels can be observed with dimensions of about 11.466 × 9.235 Å (Figure 5), and along the *c* axis, the channels show honeycomb shape with dimensions of about 7.387 × 5.173 Å (Figure 6) with the guest 4,4′-bipy molecules and water molecules residing in the channels.

It is also striking that the structure of compound **1** exhibits extensive hydrogen-bonding interactions among water molecules, 4,4′-bipy groups, and polyoxoanions. The typical hydrogen bonds are C(10)···O(10) = 3.288 Å, C(18)···O(4) = 3.210 Å, OW(1)···OW(3) = 2.605 Å, and OW(5)···O(12) = 2.768 Å (Table S1). It is believed that the extensive hydrogen-bonding interactions play an important role in the stabilization of the 3D supramolecular architecture.

When the bidentate ligands of phen and 2,2′-bipy were used instead of 4,4′-bipy, we got two analogous bisupported structures of **2** and **3** under similar reaction conditions. Compound **2** is constructed from $[(ZnO_6)(As_3O_3)_2Mo_6O_{18}]^{4-}$ anions, zinc−phen coordination complexes, and water molecules (Figure 7). Zn(2) is in the center of a distorted octahedron, which is defined by four nitrogen atoms of two phen ligands, a terminal oxo group of the $[(ZnO_6)(As_3O_3)_2Mo_6O_{18}]^{4-}$ cluster, and a water molecule. It is noteworthy that each $[(ZnO_6)(As_3O_3)_2Mo_6O_{18}]^{4-}$ unit acts as a bidentate ligand coordinating to two $\{Zn(phen)_2(H_2O)\}$ subunits via the terminal oxygen atoms of two opposite MO_6 octahedra to generate the bisupported structure (Figure 9a). The adjacent bisupported structures are stably packed together and exhibit a 3D supramolecular architecture (Figure S3) via hydrogen bonding (Table S2) and aromatic $\pi-\pi$ stacking interactions among water molecules, phen groups, and polyoxoanions.

Compound **3** is built up of $[(ZnO_6)(As_3O_3)_2Mo_6O_{18}]^{4-}$ anions, zinc-2,2′-bipy coordination complexes, and water

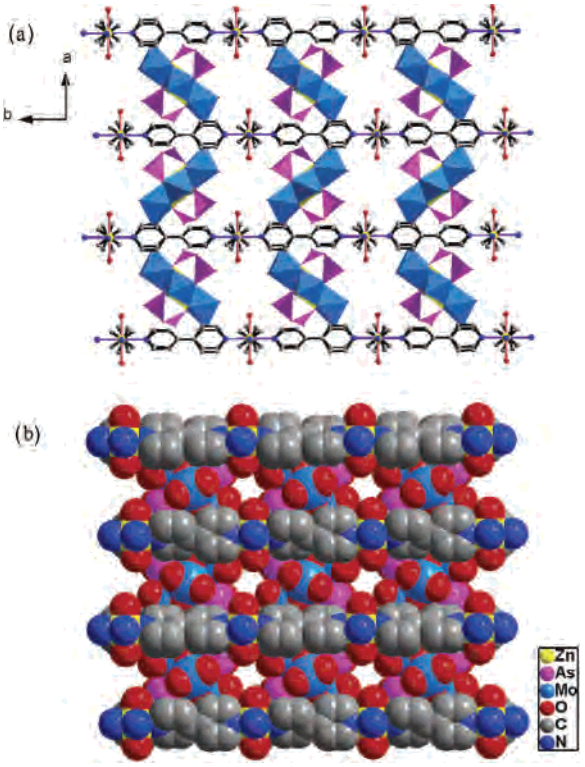

Figure 6. (a) Polyhedral and ball-stick representation of the 3D supramolecular structure of **1** along the *c* axis. (b) Space-filling diagram of the 3D supramolecular channel framework structure of **1** along the *c* axis. Lattice water molecules and free organic molecules have been omitted for clarity.

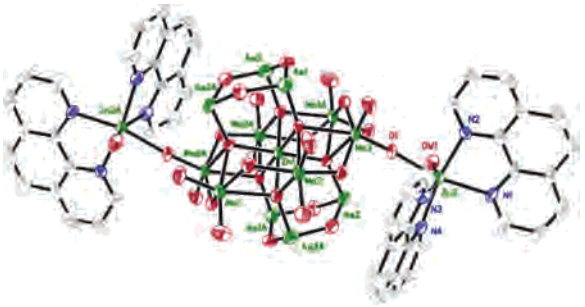

Figure 7. ORTEP drawing of **2** with thermal ellipsoids at 50% probability. The lattice water molecules have been omitted for clarity.

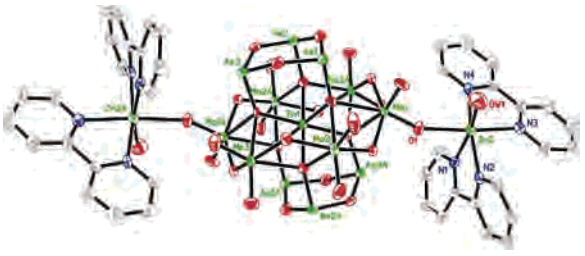

Figure 8. ORTEP drawing of **3** with thermal ellipsoids at 50% probability. The lattice water molecules have been omitted for clarity.

molecules (Figure 8). Zn(2) is defined by four nitrogen atoms of two 2,2′-bipy ligands, a terminal oxygen atom of the $[(ZnO_6)(As_3O_3)_2Mo_6O_{18}]^{4-}$ cluster, and a terminal ligand water molecule to complete an octahedral coordination environment. Each zinc coordination complex fragment $[Zn(2,2'\text{-bipy})_2(H_2O)]^{2+}$ is bonded to the terminal oxygen atoms of two opposite octahedral molybdenum sites of the

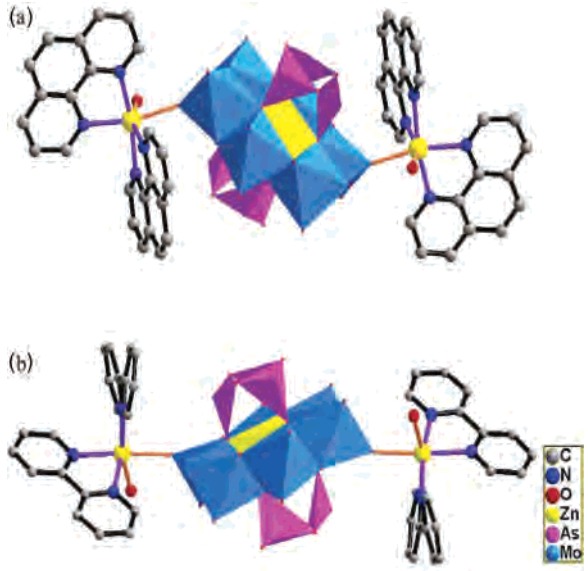

Figure 9. (a) Polyhedral and ball-stick representation of the bisupported structure of **2**. (b) Polyhedral and ball-stick representation of the bisupported structure of **3**. The lattice water molecules have been omitted for clarity.

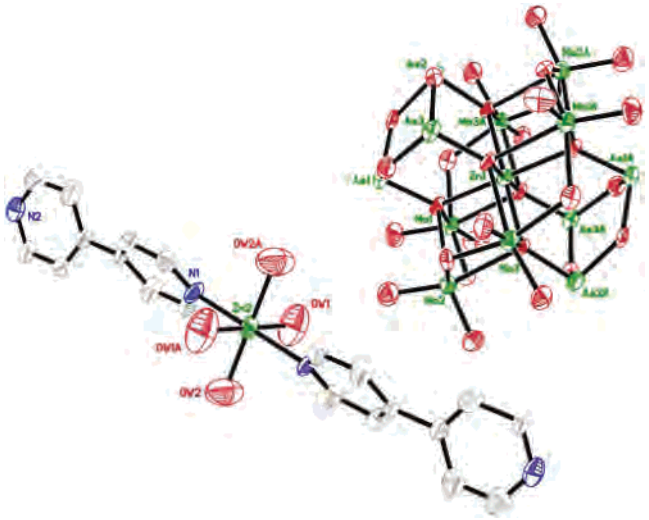

Figure 10. ORTEP drawing of **4** with thermal ellipsoids at 50% probability. The lattice water molecules have been omitted for clarity.

$[(ZnO_6)(As_3O_3)_2Mo_6O_{18}]^{4-}$ anion to form the bisupported structure (Figure 9b). The adjacent bisupported structures are stably packed together and also exhibit a 3D supramolecular architecture (Figure S4) via hydrogen bonding (Table S3) and aromatic $\pi-\pi$ stacking interactions among water molecules, 2,2′-bipy groups, and polyoxoanions.

When 4,4′-bipy ligands were used at a lower pH value, we got compound **4**. Compound **4** consists of the $[(ZnO_6)(As_3O_3)_2Mo_6O_{18}]^{4-}$ anion, protonated zinc coordination complexes, and lattice water molecules (Figure 10). The $[(ZnO_6)(As_3O_3)_2Mo_6O_{18}]^{4-}$ unit is a discrete cluster. Zn(2), residing in a distorted octahedron, is coordinated to four water molecules and two nitrogen atoms of two 4,4′-bipy ligands. According to the consideration of the charge balance and weak acidic conditions of the synthesis, the coordinated 4,4′-bipy groups are protonated. The protonated zinc coordition complexes have a dual role: charge-balance and structure direction via hydrogen bonds. Compound **4** exhibits

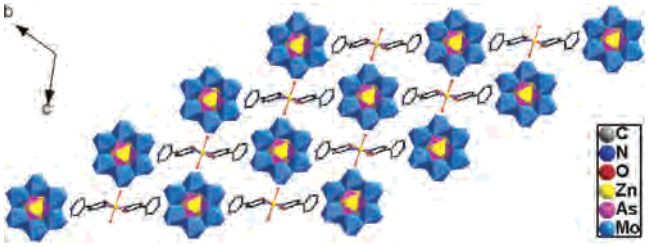

Figure 11. Polyhedral and ball-stick representation of the 3D supramolecular framework structure of **4** along the *a* axis.

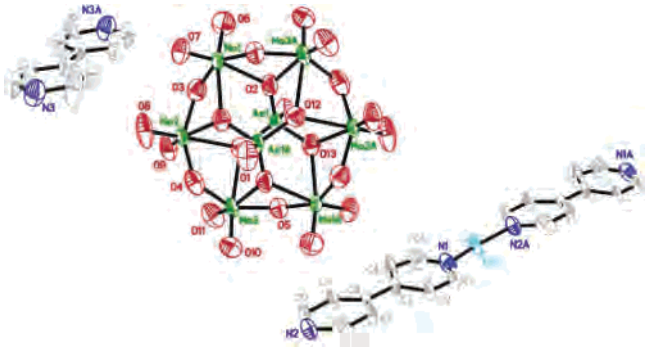

Figure 12. ORTEP drawing of **5** with thermal ellipsoids at 50% probability. The lattice water molecules have been omitted for clarity.

extensive hydrogen-bonding interactions (Table S4) among 4,4′-bipy groups, water molecules, and polyoxoanions to form a 3D supramolecular architecture (Figure 11).

Structural Analyses of 5−8. The $[H_xAs_2Mo_6O_{26}]^{(6-x)-}$ cluster was first reported in 1888.[1a] Pettersson[1a] put forward a D_{3d} structure similar to α-$[Mo_8O_{26}]^{4-}$, that is, two $\{AsO_4\}$ tetrahedra were capped with the opposing faces of a Mo_6O_6 ring, which was constructed from six $\{MoO_6\}$ octahedra linked to each other in the edge-sharing mode. In 1977, Pope's group[14] proved the above-mentioned structure by X-ray diffraction analyses and further characterized the two isomers of $[H_xAs_2Mo_6O_{26}]^{(6-x)-}$, namely, A-type and B-type in the complexes $[N(CH_3)_4]_2Na_2[(CH_3AsO_3)_2Mo_6O_{18}]\cdot 6H_2O$ and $[(CN_3H_6)_4][(C_6H_5AsO_3)_2MO_6O_{19}H_2]\cdot 4H_2O$. However, the above compounds were both synthesized with organic arsenic reagent. To date, the use of the inorganic polyanions $[H_xAs_2Mo_6O_{26}]^{(6-x)-}$ to construct the extended structure remained rare.[16a]

Compound **5** represents the first example of ribbon structure based on inorganic molybdearsenate clusters $[H_xAs_2Mo_6O_{26}]^{(6-x)-}$. Compounds **6**−**8** exhibit three isomers of $[H_xAs_2Mo_6O_{26}]^{(6-x)-}$, that is, A-isomer, B-isomer, and B′-isomer, which are all prepared with inorganic arsenate reagent. Furthermore, compound **8** displays a new isomer B′-$[As_2Mo_6O_{26}(H_2O)]^{6-}$.

Compound **5** possesses a 1D infinite ribbon structure composed of parallel copper coordination complex chains connected by $[H_2As^V{}_2Mo_6O_{26}]^{4-}$ clusters via weak Cu−O interactions. Compound **5** is made up of A-$[H_2As_2Mo_6O_{26}]^{4-}$ clusters, copper-4,4′-bipy coordination complexes, free protonated 4,4′-bipy molecules, and lattice water molecules (Figure 12). Three kinds of oxygen atoms exist in the $[H_2As_2Mo_6O_{26}]^{4-}$ cluster, that is, the terminal oxygen O_t, double-bridging oxygen $O(\mu_2)$, three-bridging oxygen $O(\mu_3)$.

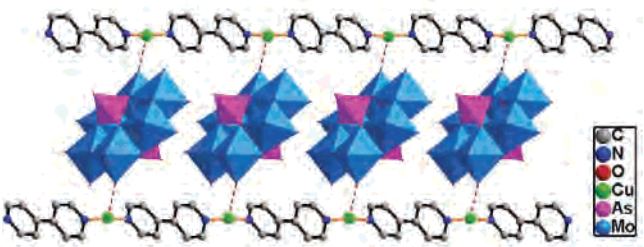

Figure 13. Polyhedral and ball-stick representation of the 1D ribbon structure of **5**. The lattice water molecules and free 4,4′-bipy molecules have been omitted for clarity.

Thus the Mo−O bond lengths can be grouped into three sets: Mo−O_t = 1.665(13)−1.736(12) Å, Mo−O(μ_2) = 1.872(11)−1.941(13) Å, and Mo−O(μ_3) = 2.314(10)-2.419-(12) Å. The As−O bond lengths fall into two classes: As−O_t = 1.685(9) Å and As−O(μ_3) = 1.622(12) and 1.723(10) Å. There is one crystallization-independent copper atom in compound **5**. Cu(1), residing in a linear geometry, is defined by two nitrogen donors from two 4,4′-bipy ligands (Cu(1)−N(1) = 1.926(13) Å and Cu(1)−N(2)#1 = 1.920(14) Å). The bond valence sum calculations indicate that the Cu sites are in the +1 oxidation state, confirmed by the particular coordination environments of Cu(I) ions. Little crystallographic disorder can be observed for Cu(1). Each copper atom acts as a linker, which is coordinated with 4,4′-bipy molecules to yield 1D chains. The two parallel running chains are connected by $[H_2As_2Mo_6O_{26}]^{4-}$ via weak Cu^I−O interactions to form an infinite 1D ladderlike ribbon along the *a* axis (Figure 13). According to the consideration of the charge balance and weak acidic condition of the synthesis, the free 4,4′-bipy groups are protonated.

The adjacent chains are stably packed together and exhibit 3D supermolecular arrays with channels (Figures S5−S8) via extensive hydrogen-bonding interactions (Table S5) among water molecules, 4,4′-bipy groups, and polyoxoanions. The elliptical shape channels along the *b* axis can be observed with dimensions of about 11.04 × 4.83 Å (Figure 14). Free 4,4′-bipy ligands and water molecules are located in these channels.

Compound **6** consists of discrete cluster $[H_2As_2Mo_6O_{26}]^{4-}$, protonated 4,4′-bipy molecules, and lattice water molecules (Figure 15). The polyanion $[H_2As_2Mo_6O_{26}]^{4-}$ is an A-type isomer, which be described as a Mo_6O_6 ring capped on opposite faces by tripodal $\{AsO_4\}$ tetrahedra. The Mo_6O_6 ring is constructed from six $\{MoO_6\}$ octahedra linked with each other by edge-sharing. Each capped $\{AsO_4\}$ tetrahedron is linked to $\{MoO_6\}$ octahedra via corner-sharing (Figure 18a). Three kinds of oxygen atoms exist in the cluster according to the manner of oxygen coordination: the terminal oxygen O_t, double-bridging oxygen O(μ_2), and three-bridging oxygen O(μ_3). Thus the Mo−O bond lengths fall into three classes: Mo−O_t = 1.708(2)−1.712(2) Å, Mo−O(μ_2) = 1.8949(13)−1.903(2) Å, and Mo−O(μ_3) = 2.3421(19)−2.3754(18) Å. The As−O bond lengths fall into two classes: As−Ot = 1.703(2) Å and As−O(μ_3) = 1.692(2)−1.6959(19) Å. When the charge balance and acidic conditions of the synthesis are considered, free 4.4′-bipy molecules are protonated.

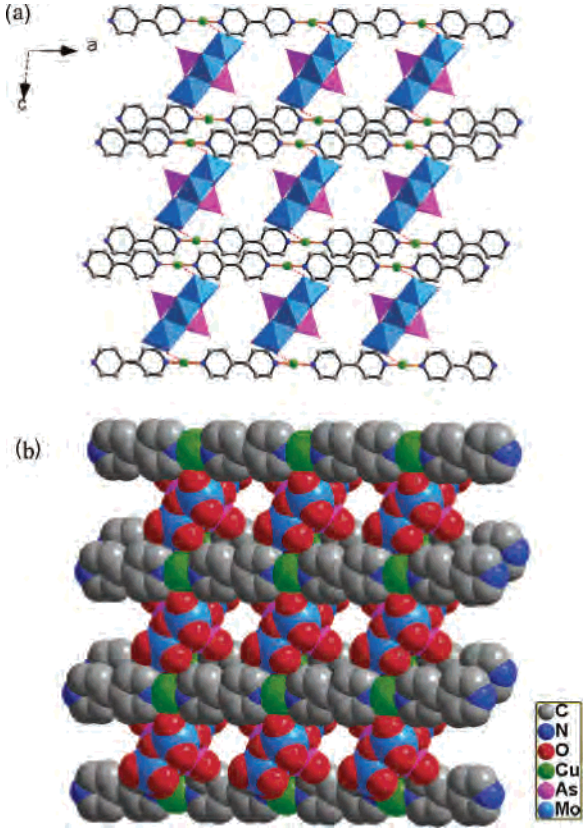

Figure 14. (a) Polyhedral and ball-stick representation of the 3D supramolecular framework structure of **5** along the *b* axis. (b) Space-filling diagram of the 3D supramolecular channel framework structure of **5** along the *b* axis. The lattice water molecules and free 4,4′-bipy molecules have been omitted for clarity.

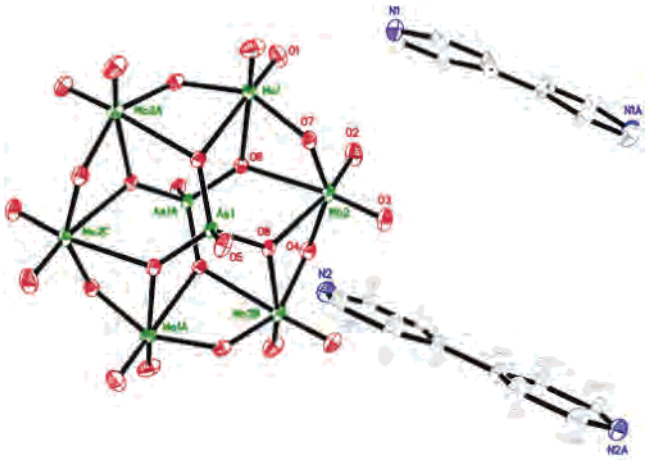

Figure 15. ORTEP drawing of **6** with thermal ellipsoids at 50% probability. The lattice water molecules have been omitted for clarity.

Compound **7** is constructed from discrete cluster $[H_2As_2Mo_6O_{26}(H_2O)]^{4-}$, protonated 4,4′-bipy molecules, and lattice water molecules (Figure 16). The $[H_2As_2Mo_6O_{26}(H_2O)]^{4-}$ cluster is a B-type isomer, which also consists of a Mo_6O_6 ring capped on opposite faces by tripodal $\{AsO_4\}$ tetrahedra. Unlike the A-type isomer, in the Mo_6O_6 ring, two $\{MoO_6\}$ octahedra share a face via a μ_2-oxo group, a μ_3-oxo group,

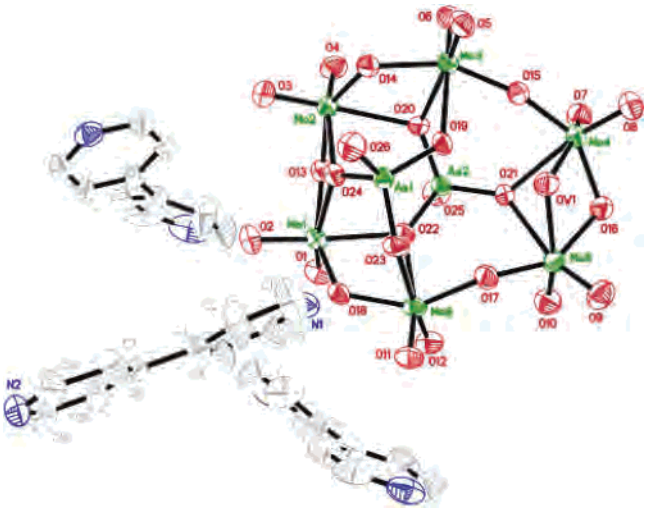

Figure 16. ORTEP drawing of **7** with thermal ellipsoids at 50% probability. The lattice water molecules have been omitted for clarity.

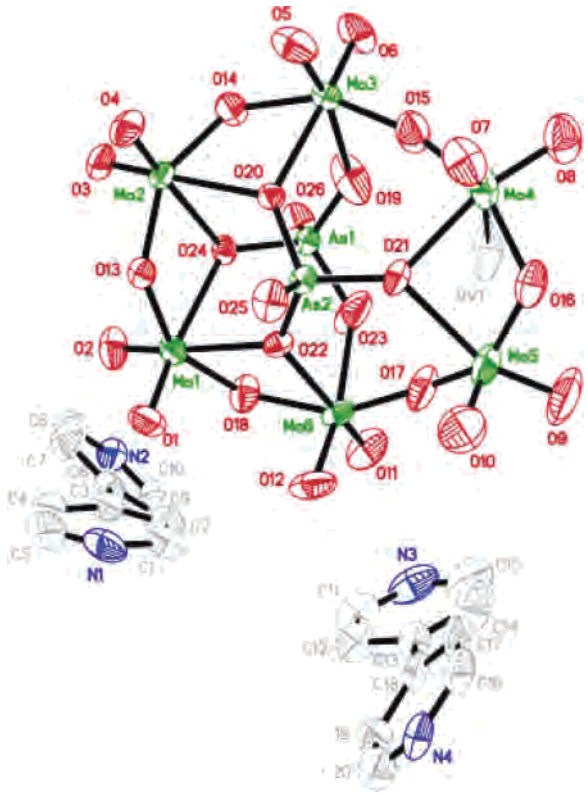

Figure 17. ORTEP drawing of **8** with thermal ellipsoids at 50% probability. The lattice water molecules have been omitted for clarity.

and a μ_2-H_2O to form a $\{Mo_2O_9H_2\}$ moiety, which links to four edge-sharing $\{MoO_6\}$ octahedra via corner-sharing (Figure 18b). It is noticeable that the B-type isomer contains a μ_2-H_2O group, which is still rare in Mo−O clusters. Four kinds of oxygen atoms exist in the cluster according to the manner of oxygen coordination: the terminal oxygen O_t, double-bridging oxygen $O(\mu_2)$, three-bridging oxygen $O(\mu_3)$, and double-bridging water molecule $H_2O(\mu_2)$. Thus the Mo−O bond lengths fall into four classes: $Mo-O_t = 1.691(4)-1.724(4)$ Å, $Mo-O(\mu_2) = 1.864(3)-2.302(3)$ Å, $Mo-O(\mu_3) = 2.232(3)-2.398(3)$ Å, and $Mo-H_2O(\mu_2) = 2.296(3)-2.320(4)$ Å. The As−O bond lengths fall into three

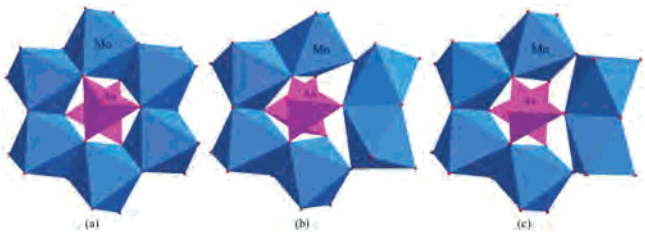

Figure 18. Polyhedral representation of three isomers of $[H_xAs_2Mo_6O_{26}]^{(6-x)-}$: (a) A-$[As^V_2Mo_6O_{26}]^{6-}$, (b) B-$[As^V_2Mo_6O_{26}(H_2O)]^{6-}$, and (c) B′-$[As^V_2Mo_6O_{26}(H_2O)]^{6-}$.

classes: $As-O_t = 1.689(3)-1.713(3)$ Å, $As-O(\mu_2) = 1.669(3)$ and $1.670(3)$ Å, and $As-O(\mu_3) = 1.670(3)-1.689(3)$ Å. According to the charge balance and acidic conditions of the synthesis, the free 4,4′-bipy molecules are protonated. To the best of our knowledge, compound **7** represent the first example of B-type inorganic cluster $[H_2As_2Mo_6O_{26}(H_2O)]^{4-}$.

Compound **8** is composed of discrete cluster B′-$[H_2As_2Mo_6O_{26}(H_2O)]^{4-}$, protonated 4,4′-bipy ligands, and lattice water molecules (Figure 17). The polyanion $[H_2As_2Mo_6O_{26}(H_2O)]^{4-}$ is a new isomer, which also consists of a Mo_6O_6 ring capped on opposite faces by tripodal $\{AsO_4\}$ tetrahedra. In contrast with the A and B-type isomers, the Mo_6O_6 ring consists of five $\{MoO_6\}$ octahedra and one $\{MoO_5\}$ square pyramid. In the Mo_6O_6 ring, one $\{MoO_6\}$ octahedron and one $\{MoO_5\}$ square pyramid share an edge via a μ_3-oxo group and a μ_2-oxo group to yield a $\{Mo_2O_9\}$ moiety, which links to four edge-sharing $\{MoO_6\}$ octahedra via corner sharing (Figure 18c). To the best of our knowledge, it is the first example of polyanion $[H_xAs_2Mo_6O_{26}]^{(6-x)-}$containing molybdenum atoms with two types of coordination modes. Little crystallographic disorder can be observed for O5 and O7. It is interesting that the Mo(2) atom is coordinated by five oxygen atoms and one water molecule (Mo(2)−OW1 = 2.468(7) Å); such a coordination mode is infrequent in the system of Mo−O clusters. Four kinds of oxygen atoms exist in the cluster according to the manner of oxygen coordination: the terminal oxygen O_t, double-bridging oxygen $O(\mu_2)$, three-bridging oxygen $O(\mu_3)$, and water molecules. Thus the Mo−O bond lengths fall into four classes: $Mo-O_t = 1.681(8)-1.710(7)$ Å, $Mo-O(\mu_2) = 1.866(6)-2.246(13)$ Å, $Mo-O(\mu_3) = 2.234(6)-2.356(5)$ Å, and Mo(2)−OW1 = 2.468(7) Å. The As−O bond lengths fall into three classes: $As-O_t = 1.663(5)$ and $1.700(5)$ Å, $As-O(\mu_2) = 1.607(10)$ and $1.71(13)$ Å, and $As-O(\mu_3)$ $1.685(5)-1.694(5)$ Å. According to the charge balance and acidic conditions of the synthesis, the free 4,4′-bipy groups and partial free water molecules are protonated.

The bond valence sum calculations[23] indicate that all Zn sites are in the +2 oxidation state, all Mo sites are in the +6 oxidation state, and all As sites are in the +3 oxidation state in compounds **1**−**4**. Cu sites are in the +1 oxidation state in compound **5.** All Mo sites are in the +6 oxidation state, and all As sites are in the +5 oxidation state in compounds **5**−**8**.

XPS Spectroscopy. The XPS spectra of compound **2** (Figure S10) in the energy regions of Zn_{2p}, Mo_{3d}, and As_{3d}

(23) Brown, I. D.; Altermatt, D. *Acta Crystallogr.* **1985**, *B41*, 244.

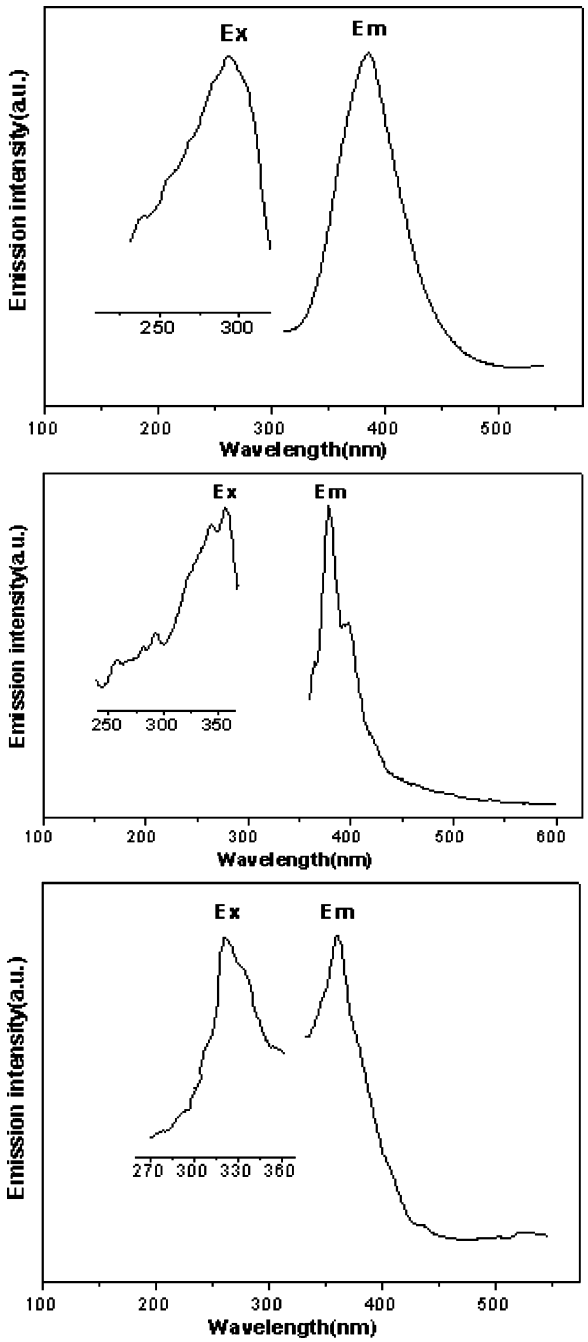

Figure 19. (a) Solid-state emission spectra of compound **1** at room temperature. (b) Solid-state emission spectra of compound **2** at room temperature. (c) Solid-state emission spectra of compound **3** at room temperature.

show peaks at 1021.4, 232.1, and 44.1 eV, respectively, attributable to Zn^{2+}, Mo^{6+} and As^{3+}. These results further confirm the valences of compound **2**.

Photoluminescence Spectroscopy. The emission spectra of compounds **1**−**3** in the solid state at room temperature are depicted in Figure 19. It can be observed that intense emissions occur at 386 nm (Figure 19a, λ_{ex} = 290 nm) for **1**, 378 and 397 nm (Figure 19b, λ_{ex} = 340 nm) for **2**, and 362 nm (Figure 19c, λ_{ex} = 320 nm) for **3**. To understand the nature of the emission band, the photoluminescence properties of the free ligands were analyzed, and we found that similar emissions (λ_{em}= 415 nm for 4,4′-bipy, 362 and 380 nm for phen, and 360 nm for 2,2′-bipy) could be observed for free ligands (Figure S9). Therefore, the emissions of **1**−**3** may be assigned to the intraligand fluorescent emission. These observations indicate that compounds **1**−**3** may be excellent candidates for potential solid-state photofunctional materials, since these condensed materials are thermally stable and insoluble in common polar and nonpolar solvents.

FT-IR spectroscopy. In the IR spectrum of compound **1** (Figure S11a), the characteristic peaks at 944, 887, 813, 779, 744, 654, and 642 cm^{-1} are assignable to the ν(Mo═O), ν-(Mo−O−M), and ν(As−O) (M = Mo or As) stretches. Bands in the 1619−1072 cm^{-1} region are attributed to the 4,4′-bipy groups. The peak at 3334 cm^{-1} is assigned to the water molecules. In the IR spectrum of compound **2** (Figure S11b), the characteristic peaks at 935, 905, 887, 866, 850, 814, 798, 725, and 671 cm^{-1} correspond to the ν(Mo═O), ν(Mo−O−M), and ν(As−O) (M = Mo or As) stretches. Bands in the 1625−1103 cm^{-1} region are attributed to the phen groups. The peak at 3370 cm^{-1} is as signed to the water molecules. In the IR spectrum of compound **3** (Figure S11c), the characteristic peaks at 933, 902, 874, 808, 778, 737, 678, and 650 cm^{-1} correspong to the ν(Mo═O), ν(Mo−O−M), and ν(As−O) (M = Mo or As) stretches. Bands in the 1596−1248 cm^{-1} region are attributed to the 2,2′-bipy groups. The peak at 3429 cm^{-1} is assigned to the water molecules. In the IR spectrum of compound **4** (Figure S11d), the characteristic peaks at 951, 933, 890, 863, 815, 781, 734, 676, and 641 cm^{-1} correspond to the ν(Mo═O), ν(Mo−O−M), and ν(As−O) (M = Mo or As) stretches. Bands in the 1613−1073 cm^{-1} region are attributed to the 4,4′-bipy groups. The peak at 3447 cm^{-1} is assigned to the water molecules. In the IR spectrum of compound **5** (Figure S12a), the characteristic peaks at 948, 897, 864, 811, 726, and 665 cm^{-1} correspond to the ν(Mo═O), ν(Mo−O−M), and ν(As−O) (M = Mo or As) stretches. Bands in 1612−1072 cm^{-1} region are attributed to the 4,4′-bipy groups. The peak at 3419 cm^{-1} is assigned to the water molecules. In the IR spectrum of compound **6** (Figure S12b), the characteristic peaks at 942, 895, 873, 840, 796, 680, and 666 cm^{-1} correspond to the ν(Mo═O), ν(Mo−O−M), and ν(As−O) (M = Mo or As) stretches. Bands in the 1611−1066 cm^{-1} region are attributed to the 4,4′-bipy groups. The peak at 3456 cm^{-1} is assigned to the water molecules. In the IR spectrum of compound **7** (Figure S12c), the characteristic peaks at 942, 896, 873, 840, 798, 681, and 666 cm^{-1} correspond to the ν(Mo═O), ν(Mo−O−M), and ν(As−O) (M = Mo or As) stretches. Bands in the 1612−1067 cm^{-1} region are attributed to the 4,4′-bipy groups. The peak at 3457 cm^{-1} is assigned to the water molecules. In the IR spectrum of compound **8** (Figure S12d), the characteristic peaks at 942, 895, 872, 840, 797, 680, and 666 cm^{-1} correspond to the ν(Mo═O), ν(Mo−O−M), and ν(As−O) (M = Mo or As) stretches. Bands in 1611−1067 cm^{-1} region are attributed to the 4,4′-bipy groups. The peak at 3452 cm^{-1} is assigned to the water molecules.

TG Analyses. The TG curve of compound **1** is shown in Figure S13a. The TG curve of **1** exhibits three steps of weight losses. The first weight loss is 5.27% in the temperature range

of 42−136 °C, corresponding to the release of the noncoordinated water molecules (calcd 4.7%). The second weight loss is 7.86% from 140 to 221 °C, corresponding to the release of free 4,4′-bipy molecules and coordinated water molecules (calcd 8.51%). The three step is 45.38% in the temperature range of 230−715 °C, all assigned to the loss of coordinated 4,4′-bipy molecules and As_2O_3 molecules (calcd 45.44%). It shows a total weight loss of 58.51% in the range of 44−709 °C, which agrees with the calculated value of 58.65%.

The TG curve of **2** is shown in Figure S13b. It shows a total weight loss of 57.48% in the range of 44−709 °C, which agrees with the calculated value of 56.2%. The weight loss of 4.1% at 44−197 °C corresponds to the loss of noncoordinated water molecules (calcd 2.85%). The weight loss of 53.38% at 221−709 °C arises from the loss of coordinated water molecules, phen molecules, and As_2O_3 molecules (calcd 53.35%).

The TG curve of **3** is shown in Figure S13c. It shows a total weight loss of 53.88% in the range of 44−707 °C, which agrees with the calculated value of 54.47%. The weight loss of 2.67% at 44−201 °C corresponds to the loss of noncoordinated water molecules (calcd 2.96%). The weight loss of 51.21% at 234−707 °C arises from the loss of coordinated water molecules, 2,2′-bipy molecules, and As_2O_3 molecules (calcd 51.51%).

The TG curve of **4** is shown in Figure S13d. It gives a total weight loss of 53.65% in the range of 43−876 °C, which agrees with the calculated value of 52.61%. The weight loss is 6.36% in the range of 43−195 °C, which corresponds to the loss of noncoordinated water molecules (calcd 6.65%), and then the sample keeps relatively stable in the temperature range of 195−260 °C. The weight loss of 47.29% at 260−876 °C arises from the loss of 4,4′-bipy molecules, water molecules, and As_2O_3 molecules (calcd 45.96%).

The TG curve of **5** exhibits two steps of weight losses (Figure S14a). The first weight loss is 1.84% in the range of 44−178 °C, corresponding to the release of the noncoordinated water molecules (calcd 1.02%). The second weight loss is 40.87% from 196 to 611 °C, assigned to the loss of 4,4′-bipy molecules, water molecules, As_2O_3 molecules, and partial oxygen molecules (calcd 40.71%). The whole weight loss (42.71%) is in agreement with the calculated value (41.73%).

The TG curve of **6** exhibits two steps of weight losses (Figure S14b). The first weight loss is 4.32% in the range of 44−183 °C, corresponding to the release of the noncoordinated water molecules (calcd 4.27%). The second weight loss is 44.01% from 215 to 663 °C, assigned to the loss of 4,4′-bipy molecules, water molecules, As_2O_3 molecules, and partial oxygen molecules (calcd 44.56%). The whole weight loss (48.33%) is in agreement with the calculated value (48.83%). The TG curves of compounds **7** and **8** exhibit similar weight loss stages. In **7**, the whole weight loss (48.69%) is in agreement with the calculated value (49.36%) (Figure S14c). In **8**, the whole weight loss (46.36%) is in agreement with the calculated value (45.89%) (Figure S14d).

Conclusions

In summary, we successfully synthesized a series of new molybdenum arsenate complexes constructed from $[(ZnO_6)(As_3O_3)_2Mo_6O_{18}]^{4-}$ and $[H_xAs_2Mo_6O_{26}]^{(6-x)-}$ clusters as SBUs. This work demonstrates that it is a feasible route to use molybdenum arsenates as SBUs building up functionalized open-framework solid-state materials. We expect that this will provide help for the construction of extended molybdenum arsenate frameworks based on inorganic molybdearsenate clusters and investigation with the potentinal applications of these compounds.

Acknowledgment. The authors thank the National Natural Science Foundation of China (20371011) for financial support.

Supporting Information Available: X-ray crystallographic files for compounds **1**−**8** in CIF format and additional figures and tables. This material is available free of charge via the Internet at http://pubs.acs.org.

IC061227J